Published in final edited form as:
Cancer Cell. 2014 August 11; 26(2): 222–234. doi:10.1016/j.ccr.2014.06.026.

Phosphorylation of ETS1 by Src Family Kinases Prevents its Recognition by the COP1 Tumor Suppressor

Gang Lu[1], **Qing Zhang**[1], **Ying Huang**[2], **Jiaxi Song**[3], **Ross Tomaino**[4], **Tobias Ehrenberger**[5], **Elgene Lim**[1,6], **Wenbin Liu**[7], **Roderick T. Bronson**[8], **Michaela Bowden**[2], **Jane Brock**[3], **Ian Krop**[3], **Deborah A. Dillon**[3], **Steven P. Gygi**[4], **Gordon B. Mills**[7], **Andrea L. Richardson**[3,9], **Sabina Signoretti**[1,3], **Michael B. Yaffe**[5], and **William G. Kaelin Jr.**[1,10,*]

[1]Department of Medical Oncology, Dana-Farber Cancer Institute, Boston, MA 02215, USA

[2]Center for Molecular Oncologic Pathology, Dana-Farber Cancer Institute, Boston, MA 02215, USA

[3]Department of Pathology, Brigham and Women's Hospital, Harvard Medical School, Boston, MA 02115, USA

[4]Department of Cell Biology, Harvard Medical School, Boston, MA 02115, USA

[5]Koch Institute for Integrative Cancer Research, Department of Biology, Massachusetts Institute of Technology, Cambridge, MA 02139, USA

[6]Department of Medicine, Brigham and Women's Hospital, Harvard Medical School, Boston, MA 02215, USA

[7]Department of Systems Biology, The University of Texas MD Anderson Cancer Center, Houston, TX, 77030, USA

[8]Rodent Histopathology Core, Dana Farber/Harvard Cancer Center, Harvard Medical School, Boston, MA 02115, USA

[9]Department of Cancer Cell Biology, Dana-Farber Cancer Institute, Boston, MA 02215, USA

[10]Howard Hughes Medical Institute, Chevy Chase, MD 20815, USA

Summary

Oncoproteins and tumor suppressors antagonistically converge on critical nodes governing neoplastic growth, invasion, and metastasis. We discovered that phosphorylation of the ETS1 and ETS2 transcriptional oncoproteins at specific serine or threonine residues creates binding sites for the COP1 tumor suppressor protein, which is an ubiquitin ligase component, leading to their destruction. In the case of ETS1, however, phosphorylation of a neighboring tyrosine residue by Src family kinases disrupts COP1 binding, thereby stabilizing ETS1. Src-dependent accumulation

*Correspondence: william_kaelin@dfci.harvard.edu.

of ETS1 in breast cancer cells promotes anchorage-independent growth *in vitro*and tumor growth*in vivo*. These findings expand the list of potential COP1 substrates to include proteins whose COP1-binding sites are subject to regulatory phosphorylation and provide insights into transformation by Src family kinases.

Introduction

Regulation of protein stability by ubiquitin ligase complexes plays an important role in cellular homeostasis including the control of cancer-relevant processes such as proliferation, differentiation, apoptosis, and angiogenesis. Accordingly, there are now many examples of driver mutations that alter the behavior of ubiquitin ligase complexes through alterations of their substrate recognition subunits. Examples include amplification of *MDM2* and *SKP2* and mutational inactivation of *VHL*, *FBW7*, *CBL*, and *RFWD2 (COP1)* (Lipkowitz and Weissman, 2011).

RFWD2 (COP1), hereafter referred to as *COP1*, maps to 1q25 and is deleted in some acute lymphoblastic lymphomas, melanomas, and prostate cancers (Marine, 2012). Deletion of *Cop1* in mice causes lymphoma and, when combined with *Pten* loss, promotes the development of invasive prostatic cancer (Migliorini et al., 2011; Vitari et al., 2011). The *COP1* gene product, COP1, is the substrate recognition module of an SCF-type E3 ubiquitin ligase complex that also contains DET1, DDB4, CUL4A, and RBX1 (Marine, 2012; Wei and Kaelin, 2011). A number of potential COP1 substrates have been identified including c-Jun family members, the ETS family members ETV1, ETV4, and ETV5, the transcription factor FOXO1, the metabolic regulators ACC1 and TORC2, and the p53 tumor suppressor protein (Marine, 2012; Wei and Kaelin, 2011).

Ubiquitin ligases often respond to signals that influence their catalytic activity or ability to engage substrates. For example, substrate recognition by SKP2 is linked to substrate phosphorylation (Carrano et al., 1999; Sutterluty et al., 1999; Tsvetkov et al., 1999) and by pVHL to substrate hydroxylation (Ivan et al., 2001; Jaakkola et al., 2001). Oncogene activation leads to the induction of ARF, which physically associates with MDM2 and prevents it from polyubiquitylating p53 (Matheu et al., 2008; Sherr, 2006). In summary, upstream signals are often integrated by ubiquitin ligases and transduced into changes in substrate stability.

The viral homolog (*v-Src*) of the cellular gene *SRC* played a pivotal role in the discovery of cellular oncogenes. The Src protein is a non-receptor tyrosine kinase that has membrane-associated, cytosolic, and nuclear targets (Mayer and Krop, 2010; Summy and Gallick, 2003). Other members of the Src family include Yes, Fyn, Fgr, Lck, Hck, Blk, and Frk. *SRC* is overexpressed in a variety of tumors and, in model systems, contributes to several hallmarks of cancer including mitogen-independent growth, invasion, and metastasis (Mayer and Krop, 2010; Summy and Gallick, 2003). How, mechanistically, Src family kinases promote transformation is still incompletely understood.

Results

Polyubiquitylation of ETS2 by COP1

To identify COP1 substrates we infected HCT116 colorectal cancer cells with a lentivirus encoding FLAG-HA-COP1, which was then recovered and purified by sequential anti-FLAG and anti-HA immunopurifications. Bound proteins were eluted with FLAG and HA peptides, respectively. Proteins in the HA eluates were precipitated with trichloroacetic acid and identified by mass spectrometry. Aliquots of the eluates and flow throughs were also analyzed by SDS-polyacrylamide gel electrophoresis followed by silver staining (Figure 1A). Parental HCT116 cells were similarly processed in parallel as negative controls.

Using this approach we detected a number of proteins that associate with COP1, including components of the core COP1 ubiquitin ligase complex, such as DET1, DDB1, and DDA1, as well as proteins believed to regulate COP1 function, such as MVP and TRIB1 (Figure 1B). In addition, we detected the known COP1 substrate JunB as well as multiple ETS family members, including ETV1, ETV4, ETV5, and ETS2 (Figure 1B). Recovery of the core COP1 ligase complex components Cul4A, DDB1, DET1, together with ETV5, ETS2, and the canonical COP1 substrate c-Jun, was confirmed by western blot analysis (Figure 1C).

While this work was in progress Dixit and coworkers reported that ETV1, ETV4, and ETV5 are polyubiquitylated by COP1 (Vitari et al., 2011). We therefore focused our attention on ETS2. ETS2 contains two colinear sequences loosely conforming with the COP1 degron motif (D/E)-(D/E)-(X)-X-X-V-P-(D/E) (Figures 1D; S1A and S1B available online). We noticed that in these two putative degrons, several positions that are normally occupied by aspartic acid or glutamic acid are instead occupied by serine or threonine. These ETS2 residues, however, if phosphorylated, would supply the negative charges normally provided by aspartic acid or glutamic acid. In fact, ETS2 Ser310 has been reported to be phosphorylated by Ca(2+)/calmodulin-dependent kinase 2 (CaMKII) (Figure S1C) (Yu et al., 2009), and we confirmed this phosphorylation event in 293FT human embryonic kidney cells under basal conditions (Figure S1D).

We therefore transiently transfected 293FT cells with a plasmid encoding wild-type ETS2-HA or ETS2-HA variants in which the VP residues of either the N-terminal (VPAA1) or C-terminal (VPAA2) motifs were replaced with alanines respectively. The abundance of wild-type ETS2, as well as the VPAA1 and VPAA2 variants, was diminished in cells cotransfected to overproduce COP1 and its partner DET, but increased in cells cotransfected to produce a dominant-negative version of COP1 (COP1AE7) (Savio et al., 2008)and DET1 (Figure 1D). In contrast, the abundance of the ETS2 variant lacking both motifs (VPAA1&2) was unaffected by COP1 (Figure 1D).

In a complementary set of experiments, we infected 293FT cells with a lentivirus encoding a doxycycline (DOX)-inducible shRNA against COP1 and then superinfected these cells with a lentivirus encoding the HA-tagged ETS2 variants described above under the control of a weak (Ubc) promoter (Qin et al., 2010). Wild-type ETS2, VPAA1, and VPAA2 coimmunoprecipitated with COP1 (see Figure 2D below) and were produced at low levels

that were increased upon the administration of DOX (loss of COP1) (Figure 1E). In contrast, binding of VPAA1&2 to COP1 was undetectable (See Figure 2D below) and the basal level of VPAA1&2, which was higher than that of wild-type ETS2, was not increased further by DOX (Figure 1E). The different behavior of wild-type ETS2 and VPAA1&2 in these assays was mirrored by changes in their stability in the presence or absence of COP1 (Figure S1E). Moreover, COP1 promoted the polyubiquitylation of ETS2, but not VPAA1&2, both in vitro (Figure 1F) and in vivo (Figures 1G and S1F). Collectively, these results indicate that ETS2, like other ETS family members, is a COP1 substrate.

Tyrosine Phosphorylation Prevents the Recognition of ETS1 by COP1

We noticed that the ETS2 paralog ETS1 contains a colinear sequence that is very similar to the C-terminal COP1 degron we identified in ETS2 and that this sequence, like its ETS2 counterpart, is invariant across a number of mammals, including rodents (Figures 2A, 2B and S1A). Furthermore, Ser282 in ETS1 is, like its counterpart in ETS2 (Ser310), phosphorylated by CaMKII (Figure S2A) (Cowley and Graves, 2000; Rabault and Ghysdael, 1994). As predicted from this knowledge, COP1 promoted the polyubiquitylation of wild-type ETS1, but not an ETS1 variant in which the canonical VP residues within this putative degron were converted to alanines (ETS1 VPAA), in vitro (Figure 2C). Unexpectedly however, ETS1, in contrast to ETS2, did not bind to COP1 *in vivo* (Figure 2D) and was not stabilized in cells upon COP1 loss (Figure 2E). Note that in Figure 2D the cells were pretreated with MG132 to facilitate the detection of the COP1-ETS complexes.

We reasoned that this paradox might relate to the replacement of the phenylalanine residue in the ETS2 sequence with a tyrosine residue (Tyr283) in the ETS1 sequence, which others have reported (Mayya et al., 2009), and we confirmed, is phosphorylated *in vivo* (Figure S2A-D), and that phosphotyrosine might disrupt the interaction with COP1. To model this, we first synthesized biotinylated peptides corresponding to the potential COP degron within ETS1. As this degron contains two potential serine phosphorylation sites (residues 276 and 282), in addition to the potential tyrosine phosphorylation site, we synthesized 8 peptides corresponding to every possible combination of phosphorylation marks (Figure 3A). An additional peptide corresponding to the VPAA variant was included as a negative control (Figure 3A). These peptides, immobilized on NeutrAvidin agarose, were then used as affinity reagents to capture COP1 from 293FT cell extracts. COP1 bound, albeit weakly, to the wild-type, unphosphorylated, peptide (peptide 1) but not to the VPAA peptide (peptide 9) (Figure 3A). Furthermore, as predicted, phosphorylation of either serine residue enhanced the binding to COP1 (compare peptides 3, 5, and 7 to peptide 1). Importantly, tyrosine phosphorylation decreased binding to COP1 when combined with phosphorylation of the serine corresponding to Ser282 (compare peptide 6 to 5 and 8 to 7). These results support that tyrosine phosphorylation decreases the binding affinity of COP1 for ETS1.

To ask if this might also be true in cells, we stably infected 293FT cells with lentiviruses encoding HA-ETS1, or variants thereof, under the control of the Ubc promoter and scored their ability to capture endogenous COP1 in cells treated with MG132. Very low levels of COP1 were recovered with either wild-type COP1 (WT) or the VPAA (V280A/P281A) COP1 variant (Figure 3B, lanes 2 and 3), suggesting that this level of recovery reflects

background noise in this assay or that ETS1 has a second, low-affinity, COP1-binding site. Importantly, replacement of tyrosine 283 with phenylalanine (Y283F) dramatically enhanced the recovery of COP1 (compare lane 4 to 2). Phosphorylation of ETS1 Ser282 was confirmed using a phosphospecific antibody (Figure 3B). The signal obtained with this antibody was variably slightly diminished when examining ETS1 mutants in which Tyr283 was converted to phenylalanine, possibly due to slightly lowered antibody binding affinity to the corresponding phosphopeptides (Figure S2E).

We also tested ETS1 Y283F variants in which Ser276 and Ser282 were changed to either aspartic acid or alanine in attempt to mimic phosphorylation or loss of phosphorylation, respectively. As expected, converting these serines to alanine abrogated COP1 binding by the Y283F variant (compare lane 6 to lane 4, lane 10 to lane 4, and lane 12 to lane 4). In contrast, replacing either Ser276 or Ser282 with aspartic acid enhanced binding (compare lanes 7 and 8 to 4 and lanes 8, 9 and 11 to lane 12), especially in combination (compare lane 8 to lane 12). These results indicate that phosphorylation of ETS1 Ser276 and Ser282 promotes binding to COP1 while Tyr283 phosphorylation decreases binding.

In keeping with these results, the Y283F substitution grossly destabilized ETS1 relative to wild-type ETS1 unless Ser276 and Ser282 were concurrently converted to alanine residues (Figure 3C). Moreover, induction of a COP1 shRNA in 293FT cells stabilized the Y283F variant, but not wild-type ETS1 (Figure 3D). This effect was specific because it was enhanced when both Ser276 and Ser282 were converted to aspartic acid and eliminated when these two residues were converted to alanine (Figure 3D). Collectively, these results indicate that the differential effects of COP1 on ETS1 and ETS2 *in vivo* relates to the ability of ETS1 to be phosphorylated on Tyr283.

Regulation of ETS1 by Src Family Kinases

The sequence surrounding ETS1 Tyr283 resembles a Src family kinase phosphorylation motif (Figure S3A) and Src can phosphorylate ETS1 on this site in vitro (Figures S3B and S3C). As Src is a relatively promiscuous kinase in vitro, however, we proceeded to ask if Src can phosphorylate ETS1 in cells. In pilot experiments we confirmed that ~70% of the ETS1 in MDA-MB-231 breast carcinoma cells, which have high Src activity (Sanchez-Bailon et al., 2012), is tyrosine-phosphorylated (Figure S3D). Next we treated MDA-MB-231 breast carcinoma cells with a panel of small molecule kinase inhibitors and found that the Src family kinase inhibitor dasatinib decreased ETS1 protein levels compared to cells treated the Abl inhibitor imatinib, the EGFR family inhibitor lapatinib, or vehicle alone (Figure S3E). Inactivation of Src family kinases by dasatinib was confirmed by the loss of Src autophosphorylation at Tyr416 (or its equivalent in the other Src family kinases) and by decreased phosphorylation of the Src target FAK (Figure S3E). Moreover, dasatinib had minimal effects of ETS1 mRNA levels, suggesting that its effects on ETS1 were post-transcriptional (Figure S3F).

Treatment of MDA-MB-231 cells with increasing amounts of dasatinib decreased both ETS1 tyrosine phosphorylation and ETS1 abundance (Figure 4A). Downregulation of ETS1 by dasatinib was prevented by proteasomal blockade (Figure 4A) or depletion of COP1 with an inducible shRNA (Figure 4B).

Pulse-chase experiments confirmed that the effects of dasatinib reflected decreased ETS1 stability (Figure 4C). Moreover, the effects of dasatinib were enhanced by ionomycin, which activates the CaMKII that can phosphorylate ETS1 Ser282 (Cowley and Graves, 2000; Rabault and Ghysdael, 1994) (Figures 4C and S3G).

Of note, inhibition of Src activity and the downregulation of ETS1 were both detectable at nM concentrations of dasatinib (Figures 4A and 4B), although the former was more pronounced than the latter, possibly due to differences in the sensitivities of the two assays and differences in the kinetics of Src inactivation and ETS1 turnover (Figures 4C and 4D). In time-course experiments using cells treated with MG132, loss of ETS1 tyrosine phosphorylation after treatment with dasatinib led to a reciprocal increase in COP1 binding (Fig 4D and S3H).

To interrogate the importance of Tyr283 with respect to the control of ETS1 by Src family kinases, MDA-MB-231 cells were stably infected to produce ETS1-HA, ETS1 (VPAA)-HA, or ETS1 (Y283F)-HA under the control of the Ubc promoter. As expected, treatment of these cells with dasatinib decreased the tyrosine phosphorylation of wild-type ETS1 and the VPAA variant (Figure 4E). In contrast, recognition of ETS1 (Y283F) with the phosphotyrosine antibody under basal conditions was greatly diminished compared to wild-type ETS1 and VPAA and was not further diminished by dasatinib (Figure 4E). Importantly, dasatinib also increased the binding of wild-ETS to COP1 (Figure 4E). This effect was specific because the VPAA variant did not bind to COP1 while the Y283F variant constitutively bound COP1 (Figure 4E).

In a complementary set of experiments, MDA-MB-231 cells were first infected to produce the DOX-inducible COP1 shRNA and then superinfected to produce either wild-type ETS1-HA or ETS1 (Y283F) variants in which Ser276 and Ser282 were converted to aspartic acid or alanine. As expected, wild-type ETS1 was minimally affected by loss of COP1, presumably due to endogenous Src family kinase activation (Figure 4F, compare lane 5 to 4), and was downregulated with dasatinib (compare lane 6 to 4). In contrast, ETS1 (Y283F) was sensitive to COP1 loss (Figure 4F, compare lane 8 to 7) and no longer stabilized by dasatinib (compare lane 9 to 7). Also as expected, COP1-dependent turnover of ETS1 (Y283F) was enhanced by phosphomimetic mutations at Ser276 and Ser282 and completely abrogated by replacement of these two residues with alanines (Figure 4F).

To identify the relevant target(s) of dasatinib we next infected MDA-MB-231 cells with lentiviral vectors stably expressing shRNAs against either Src or the Src family kinases Fyn, Lyn, and Yes (Figure 5A). Two effective shRNAs were interrogated per gene. None of these four kinases, when downregulated in isolation, significantly altered ETS1 levels and FAK phosphorylation (Figure 5A). However, combined downregulation of Src and Yes, but not Src with Fyn or Lyn, dramatically lowered ETS1 tyrosine phosphorylation, ETS1 levels and FAK phosphorylation (Figures 5B, S4A and S4B). Moreover, expression of dasatinib-resistant versions of Src or Yes, but not their wild-type counterparts, restored ETS1 protein levels in dasatinib-treated cells without affecting ETS1 mRNA levels (Figures 5C and 5D and S3F). These results suggest that Src and Yes are redundant with respect to regulation of ETS1 stability.

Role for Src-dependent Accumulation of ETS1 in Triple Negative Breast Cancer

Both Src and ETS1 have been implicated as breast cancer oncogenes (Bendinelli et al., 2011; Bosman et al., 2010; Buggy et al., 2004; Charafe-Jauffret et al., 2006; Lincoln and Bove, 2005; Mayer and Krop, 2010; Myers et al., 2005; Mylona et al., 2006; Sanchez-Bailon et al., 2012; Span et al., 2002; Vetter et al., 2005; Zhang et al., 2011). We next surveyed ETS1 protein levels and Src family kinase activity in a panel of breast cancer cell lines. ETS1 protein levels were highest in triple negative breast cancer lines and correlated well with Src family kinase (SFK) activation, as determined using an antibody specific for SFKs phosphorylated at the tyrosine equivalent to Src 416 (Figure 5E and S4C). Moreover, ETS1 tyrosine phosphorylation and ETS1 levels fell dramatically in triple negative breast cancer cells treated with dasatinib (Figures 5F, S4D and S4E).

PKCa also reportedly regulates ETS1 levels (Lindemann et al., 2003; Vetter et al., 2005). Levels of activated PKCa did not, however, correlate with ETS1 levels across the breast cancer lines depicted in Figure 5E (Figure S4F) and shRNA-mediated downregulation of PKCa with 4 different shRNA did not affect ETS1 levels (Figure S4G).

To ask if ETS1 plays a role in Src-dependent transformation, we infected MCF10A immortalized mammary epithelial cells with a lentivirus encoding a v-Src-ER fusion protein (Hirsch et al., 2009; Iliopoulos et al., 2009; Reginato et al., 2005), which can be activated with tamoxifen, and then superinfected them with lentiviruses encoding one of three different DOX-inducible ETS1 shRNA or a control shRNA (Figure 6A). As expected, administration of tamoxifen increased Src activity, manifest as increased phosphorylation of the downstream target FAK (Figure 6A), and was associated with increased ETS1 levels and increased soft agar growth, except in those cells producing any one of three independent ETS1 shRNAs (Figures 6A and 6B). These shRNA effects were on-target because they could be rescued by concurrent expression of an ETS1 cDNA that was engineered to be shRNA-resistant (Figures S5A and S5B).

To ask if phosphorylation of ETS1 at Tyr283 is required for Src to promote soft agar growth by MCF10A cells, we generated MCF10A-v-SRC-ER cells stably expressing either an ETS1 shRNA or a control shRNA (Figure 6C and 6D). These cells were then infected with viruses encoding ETS1 shRNA-resistant versions of wild-type ETS1 or ETS1 variants bearing the Y283F mutation, VPAA mutation, or both mutations. As expected, tamoxifen treatment of cells increased the level of exogenous wild-type ETS1, but not the Y283F variant, whereas the VPAA variants were constitutively stable (Figure 6C). Moreover, wild-type ETS1 rescued v-Src mediated transformation in MCF10A cells in which endogenous ETS1 was first depleted by the ETS1 shRNA, while the Y283F variant did not unless it was rendered stable by a concurrent VPAA mutation (Figure 6D and 6E). Therefore promotion of breast cancer soft agar growth, a hallmark of transformation, by Src family kinases requires that it stabilizes ETS1.

In keeping with the results obtained in MCF10A cells, downregulation of ETS1 using two independent shRNAs in MDA-MB-231 cells significantly decreased soft agar growth, without affecting cell proliferation in vitro (Figures 7A, 7B and S6A). In a complementary set of experiments, we engineered MDA-MB-231 breast cancer cells to produce firefly

luciferase and then infected them to produce an shRNA against green fluorescent protein (GFP) or one of two shRNAs against ETS1 (shRNA number 2 or 3). These cells were then injected into the mammary fat pads of immunocompromised mice and allowed to form orthotopic tumors. Downregulation of ETS1 with either shRNA impaired tumor growth relative to cells expressing the GFP shRNA, as determined by serial bioluminescent imaging and tumor mass at necropsy, unless cells also expressed an shRNA-resistant ETS1 cDNA (Figures 7C-F, S6B-J). Therefore ETS1 promotes breast transformation *in vitro* and *in vivo*.

Next, we measured ETS1 protein levels and Src phosphorylation in human breast tumors by immunohistochemistry (Figure 7G and 7H). In 222 cores derived from 86 patients with triple negative breast cancer who underwent surgery for localized breast cancer, we found a significant correlation between ETS1 protein level and Src phosphorylation. 31 (75 cores) out of 33 tumors (82 cores) that had high Src activity, as determined by phosphorylation of Src tyrosine residue 416, also had high ETS1 protein levels. Conversely, 18 (43 cores) out of 53 tumors (140 cores) that had low or undetectable Src activity also had low level of ETS1 (Figure 7I and Table S1) ($p<0.001$). Collectively, these results support that Src activation is sufficient to promote the stabilization of ETS1, which contributes to breast cancer pathogenesis. The finding that some breast tumors with high ETS1 nonetheless had low levels of Src tyrosine 416 phosphorylation could reflect technical challenges measuring phosphoepitopes by immunohistochemistry or could signal the existence of alternative means of inducing ETS1.

Discussion

We found that the stabilities of ETS1 and ETS2, like those of the ETS family members ETV1, ETV4, and ETV5 (Vitari et al., 2011), are under the control of the COP1 ubiquitin ligase, thus expanding the linkage between the ETS family of oncogenic transcription factors and the COP1 tumor suppressor protein. COP1 inactivation has been linked to multiple cancers including human prostate cancer, which is often linked to deregulation of ETS family members (Clark and Cooper, 2009; Kumar-Sinha et al., 2008; Marine, 2012).

Notably, the COP1-binding degrons in ETS1 and ETS2, in contrast to ETV1, ETV4, and ETV5, contain serine or threonine residues in positions that are normally occupied by aspartic acid or glutamic acid in the COP1 substrates that have been well documented to date. This suggests that the number of potential COP1 substrates, based on primary sequence homology, is larger than would have been previously predicted and that some of these substrates will require priming phosphorylation events in order to generate the negative charges that would otherwise be provided by aspartic acid or glutamic acid. It will be important to determine which amino acids in the spacer element of this expanded COP1-binding motif {[DEST]-X (2,3)-V-P-[DEST]} are permissive for recognition by COP1 as well as the importance of local secondary structure.

There are many examples of substrates that must be phosphorylated in order to be recognized by their cognate ubiquitin ligases. Examples include p27, beta-catenin, and cyclin E, which are recognized by ^{SKP2}Scf, $^{\beta trcp}$SCF, and ^{Fbw7}SCF, respectively (Deshaies, 1999). In the case of ETS1, priming phosphorylation appears to be accomplished by calcium

and calmodulin-dependent kinases (CaM kinases). For example, ETS1 is rapidly phosphorylated by these enzymes upon T-cell activation (Bhat et al., 1990). This leads to decreased ETS1 protein levels as well as conformational changes that alter the dependence of ETS1 on neighboring transcription factors (Bhat et al., 1990; Cowley and Graves, 2000; Pognonec et al., 1988). Thus both the duration and the quality of the ETS1 response are potentially coregulated by CaM kinases following T-cell activation.

We also discovered that ETS1, in addition to requiring priming phosphorylation, contains a tyrosine residue that inhibits COP1 recruitment when phosphorylated by Src family kinases. Src and Yes appear, based on our studies, to be the Src-family kinases that control ETS1 in breast cancer cells, but it is possible that other Src family members assume this role in other contexts. Thus the COP1 degron within ETS1, the cellular homolog of v-ETS and a founding member of the mammalian ETS family, integrates both positively and negatively acting kinase signals. A search of the Prosite database revealed 126 human proteins containing the sequence [DEST]-X (2,3)-V-P-[DEST]-Y, suggesting that regulation by tyrosine phosphorylation might extend to other COP1 substrates (our unpublished findings). Included among these 126 proteins are the ETS family members ETV1 and ETV6 (also called TEL), the COP1-associated proteins CUL4 and TRIB1, and several tyrosine phosphatases. Preliminary experiments suggest that the motifs in ETV1 and TRIB1 can, as synthetic peptides, bind to COP1 and that their binding is diminished by tyrosine phosphorylation (our unpublished findings). Notably, some of the 126 proteins contain COP1 binding motifs that also conform with known phosphorylation motifs including PTPRG (Abl kinase), CNN2 (PGFRBkinase), MPP7 (PDGFR and Src kinases), KHDR2 (Fgr kinase), ILRL1 (EGFR kinase), and ATAD2 (EGFR, Fgr, and PDGFR kinases) (our unpublished findings).

The paradigm of degrons integrating positively and negatively acting signals probably extends to other ubiquitin ligase-substrate pairs as well. For example, YAP1 and IκBα both contain degrons that, when phosphorylated, are recognized by $^{\beta TRCP}$SCF. Phosphorylation of adjacent tyrosine residues, however, results in their stabilization, presumably by blocking the recruitment of $^{\beta TRCPS}$CF, although this has not yet been formally proven (Levy et al., 2008; Singh et al., 1996; Zhao et al., 2010).

The knowledge that priming phosphorylation of the COP1 degron within ETS1 is antagonized by phosphorylation of a neighboring tyrosine residue by Src family kinases suggests that some of the oncogenic activity of these kinases relates to activation of ETS target genes. In support of this view, earlier studies showed that increased Src activity and increased ETS1 are both features of triple negative breast cancers (Buggy et al., 2004; Charafe-Jauffret et al., 2006; Elsberger et al., 2009; Finn et al., 2011; Finn et al., 2007; Mylona et al., 2006; Tryfonopoulos et al., 2011). Our work suggests that that these two observations are linked. We found that ETS1 levels correlate with Src activity in mammary carcinoma cell lines, that inhibiting Src downregulates ETS1, and that elimination of ETS1 blunts Src's ability to promote mammary proliferation in soft agar. Interestingly, ETS1 has been linked to breast cancer pathogenesis before, where it is associated with a poor prognosis (Bosman et al., 2010; Myers et al., 2005; Mylona et al., 2006; Span et al., 2002; Zhang et al., 2011).

Dasatinib inhibits the proliferation of breast cancer cell lines, especially triple negative breast cancer lines (Finn et al., 2007; Huang et al., 2007; Kurebayashi et al., 2010; Lehmann et al., 2011; Tryfonopoulos et al., 2011). Moreover, breast cancer lines with the highest basal levels of ETS1 tended to be the most sensitive to dasatinib in these earlier reports (for example, compare Figure 5E here to Table 1 in (Finn et al., 2007)). Nonetheless, we have so far been unable to block the antiproliferative effects of dasatinib *in vitro* by eliminating COP1 or by expressing stabilized versions of ETS1 (data not shown). This suggests that the antiproliferative effects of dasatinib *in vitro* involve at least one Src target other than ETS1. In addition, Src inhibitors have thus far exhibited very modest activity in breast cancer patients (Herold et al., 2011; Mayer et al., 2011). This might reflect a failure to adequately enrich for patients whose tumors have activated Src or to achieve adequate target inhibition *in vivo*. In this regard, ETS1 might eventually serve as a predictive biomarker, as a pharmacodynamic biomarker, or perhaps both. It is also possible that failure to observe overt regressions of established tumors in breast cancer patients treated with dasatinib reflects a greater role for Src (and ETS1) in tumor invasion and metastasis than in tumor maintenance. ETS1 directly regulates a number of genes involved in invasion and metastasis, such as MMPs and integrins, and might thereby amplify the effects of Src-dependent phosphorylation of substrates such as FAK and TKS5 that also affect these processes (Hahne et al., 2005; Murphy and Courtneidge, 2011; Zhao and Guan, 2009).

The interactions of enzymes with their substrates are often transient in nature, precluding detection in coimmunoprecipitation assays. Moreover, polyubiquitylation at the hands of ligases such as the COP1 complex causes substrate destruction. We were therefore surprised that we could readily detect complexes containing COP1 and its substrates by coimmunoprecipitation from cells that had not been treated with drugs intended to block enzyme function or protein turnover. This raises the possibility that COP1 activity is, itself, subject to regulation that dictates whether bound substrates are efficiently polyubiquitylated. If true, this would imply that upstream signals impinge upon both the COP1 complex and its substrates.

Experimental Procedures

Cell Culture

293FT HEK (Invitrogen), HCT116 (ATCC), MDA-MB-231-LUC (a kind gift from Dr. Kimberly Briggs), and ATCC breast cancer cell lines MCF-7, ZR-75-1, T47D, BT-474, MDA-MB-453, SK-BR-3, BT-20, BT-549, MDA-MB-157, MDA-MB-231, MDA-MB-436, MDA-MB-468, HCC70, HCC1143, HCC1806 and HCC1937 were maintained in DMEM supplemented with 10% fetal bovine serum, 100 U/ml penicillin, and 100 μg/ml streptomycin. MCF10A-v-SRC-ER cell line was kindly provided by Dr. Dimitrios Iliopoulos (University of California at Los Angeles). MCF10A (ATCC) and MCF10A-v-Src-ER cells were maintained in DMEM/F12 growth medium containing 5% charcoal stripped horse serum, 100 U/ml penicillin, 100 μg/ml streptomycin, 20 ng/ml EGF, 0.5 μg/ml hydrocortisone, 100 ng/ml cholera toxin and 10 μg/ml Insulin. For v-Src acute activation, MCF10A and MCF10A-v-Src-ER cells were grown in assay medium [DMEM/F12 medium containing 2% charcoal-stripped horse serum, 100 U/ml penicillin,

100 μg/ml streptomycin, 0.5 μg/ml hydrocortisone, 100 ng/ml cholera toxin and 10 μg/ml Insulin] for 48 hours, and then treated with 1μg/ml 4-OH-tamoxifen for additional 6 hours. Stable cell lines were established by lentiviral infection followed by growth in media containing appropriate antibiotics (1 μg/ml puromycin, 20 μg/ml blasticidin, 800 ng/ml neomycin, or 500 μg/ml hygromycin).

Orthotopic Tumor Growth Assay

All animal experiments complied with National Institutes of Health guidelines and were approved by Dana-Farber Cancer Institute Animal Care and Use Committee. For orthotopic tumor growth assay, 5 × 105 viable MDA-MB-231-LUC tumor cells were resuspended in 40 μl growth factor-reduced Matrigel (BD Biosciences) and injected into the #4 and #9 mammary glands of 8-week old female NSG mice (Jackson Lab, Bar Harbor, Maine). Mice were sacrificed 8 weeks later to determine the tumor size. For weekly bioluminescence imaging, mice were injected intraperitoneally with 150 μg.g-1 D-luciferin in PBS. After 5 minutes, tumor burden was measured in an IVIS imaging system (Xenogen, Alameda, CA) and quantified using the LIVING IMAGE software (Xenogen). Results are presented as means (of total photon flux) ± standard error of the mean (SEM).

Immunohistochemistry

The breast cancer tissue microarray containing 89 triple negative tumors (negative for estrogen receptor, progesterone receptor, and HER2) was constructed with tissues obtained from patients who provided written informed consent under Dana Farber Cancer Institute IRB protocol 93-085. Each tumor sample was represented by 3 tissue microarray cores that, when possible, were taken from different areas of the same tumor. Immunohistochemical staining of ETS1 and phospho-Src was performed on 4-μm sections of the TMA, using the Bond Refine Detection System following the manufacturer's protocols on the Leica Bond III automated immunostainer. The sections were automatically deparaffinized, antigen retrieval was done with EDTA buffer (pH 9.0) and processed for 20 min. The slides were incubated with the antibody against ETS-1 (1G11, Mouse monoclonal, ab10936, Abcam) at a dilution of 1:100, or phospho-Src (Tyr416, Rabbit polyclonal, #2101, Cell Signal Technology) at a dilution of 1:50 for 60 min, respectively. The sections were then treated according to the streptavidin–biotin–peroxidase complex method (Bond Polymer Refine Detection, Leica Microsystems) with diaminobenzidine (DAB) as a chromogen and counterstained with hematoxylin. Tonsil tissue was used as positive controls for ETS-1, and testis tissue was used as positive controls for phospho-Src, respectively. Omission of the primary antibody was used as a negative control.

To evaluate IHC expression of ETS1 and pSrc on the TMA, we utilized a semiquantitative scoring system, whereby stain intensity and percentage tumor cell positivity were assessed by a pathologist. For each core, we assigned the percentage score of 0 (<5% tumor cell positivity), 1 (≥5% and <50% tumor cell positivity), 2 (≥50% tumor cell positivity) and the intensity score of 0 for negative, 1 for weak or moderate staining, 2 for strong staining (Merritt et. al 2008). ETS1 (cytosol), ETS1 (nuclear), pSrc(cytosol) and pSrc (membrane) were scored separately. Lastly, for ETS1 or pSrc, the overall staining intensity and percentage positivity scores generated an 8-point score. Three cases TN33, TN52 and TN59

were excluded from data analysis due to no or too few tumor cells or because all three cores were missing after sectioning. In order to correlate ETS1 and pSrc expression, we binned the individual scores for each marker and grouped them based on high and low expression levels. Statistical analysis was carried out using SPSS V.13.0. The Spearman rank correlation was used to investigate the correlation of the protein expression between ETS1 and phospho-Src. P values less than 0.05 were considered statistically significant.

Antibodies

Anti-COP1 antibody (A300-894A), anti-ETS1 antibody (A303-501A), anti-ZEB2 antibody (A302-474A), anti-V5 antibody (A190-120A), HRP conjugated anti rabbit secondary antibody (ReliaBLOT, WB120) were purchased from Bethyl. Anti-phospho-ETS1 (S282) antibody (44-1109), anti-phospho-ETS1 (S282/S285) antibody (44-1111) and anti-V5 (2F11F7) mouse mAb (37-7500) were purchased from Invitrogen. Anti-ETS2 antibody (SC-351), anti-GFP antibody (SC-9996), anti-HA antibody (SC-805) and anti-ERα antibody (SC-543) were purchased from Santa Cruz. Anti-CUL4A antibody (2699), anti-DDB1 antibody (5428S), anti c-Jun (60A8) rabbit mAb (9165), anti-phospho-FAK (Tyr576/577) antibody (3281), anti-FAK antibody (3285), anti-phospho-Src Family (Tyr416) antibody (2101S), anti-Src (32G6) rabbit mAb (2123), anti-Yes antibody (3201), anti-Fyn antibody (4023), anti-Lyn (C13F9) rabbit mAb (2796), anti-PKCα antibody (2056) anti-phospho-PKCα/β II (Thr638/641) antibody (9375), anti-PKCδ (D10E2) rabbit mAb (9616), anti-phospho-PKCδ (Thr505) antibody (9374), anti-E-Cadherin (24E10) rabbit mAb (3195), anti-N-Cadherin Antibody (4061), anti-Vimentin (D21H3) rabbit mAb (5741), anti-Claudin-1 antibody (4933), anti-β-Catenin (D10A8) rabbit mAb (8480), anti-ZO-1 (D7D12) rabbit mAb (8193), anti-Snail (C15D3) rabbit mAb (3879), anti-Slug (C19G7) rabbit mAb (9585), anti-ZEB1 (D80D3) rabbit mAb (3396), Phospho-Tyrosine mouse mAb (P-Tyr-100) (HRP Conjugate) (5465), anti-HA (6E2) mouse mAb (HRP Conjugate) (2999), anti-Myc (9B11) mouse mAb (2276) and anti-Myc (71D10) Rabbit mAb (2278) were purchased from Cell Signaling. Anti-Twist antibody (ARP37997_T100) was purchased from Aviva. Anti-HA (16B12) Mouse mAb (MMS-101P) was purchased from Covance. Rabbit anti-FLAG antibody (F2425), mouse anti-FLAG M2 antibody (F-3165), anti-FLAG M2 (HRP conjugate) (A8592) and anti-Vinculin antibody (V9131) were purchased from Sigma. Anti-ETV5 (7C10) mouse mAb (H00002119-M02) was purchased from Abnova. Anti-DET1 (4123) mouse mAb and anti-COP1 (4466) mouse mAb were kindly provided by Dr. Vishva Dixit (Genentech). Peroxidase-conjugated goat anti-mouse secondary antibody (31430) and peroxidase conjugated goat anti-rabbit secondary antibody (31460) were purchased from Thermo.

Supplementary Material

Refer to Web version on PubMed Central for supplementary material.

Acknowledgments

The authors thank Drs. Todd Golub, William Hahn, Kimberly Briggs and Sungwoo Lee for providing reagents, Drs. Brian D. Lehmann, Melinda E. Sanders and Jennifer A. Pietenpol for advice and technical assistance on the immunohistochemical studies, and Dr. Wenyi Wei and members of Kaelin Laboratory for helpful discussions. G.L.

is supported by the Ruth L. Kirschstein NRSA postdoctoral fellowhip award. W.G.K. is an HHMI investigator and is supported by grants from NIH, HHMI, and the Breast Cancer Research Foundation.

References

Bendinelli P, Maroni P, Matteucci E, Desiderio MA. Comparative role of acetylation along c-SRC/ETS1 signaling pathway in bone metastatic and invasive mammary cell phenotypes. Biochimica et biophysica acta. 2011; 1813:1767–1776. [PubMed: 21741415]

Bhat NK, Thompson CB, Lindsten T, June CH, Fujiwara S, Koizumi S, Fisher RJ, Papas TS. Reciprocal expression of human ETS1 and ETS2 genes during T-cell activation: regulatory role for the protooncogene ETS1. Proceedings of the National Academy of Sciences of the United States of America. 1990; 87:3723–3727. [PubMed: 2187191]

Bosman JD, Yehiely F, Evans JR, Cryns VL. Regulation of alphaB-crystallin gene expression by the transcription factor Ets1 in breast cancer. Breast Cancer Res Treat. 2010; 119:63–70. [PubMed: 19205872]

Buggy Y, Maguire TM, McGreal G, McDermott E, Hill AD, O'Higgins N, Duffy MJ. Overexpression of the Ets-1 transcription factor in human breast cancer. Br J Cancer. 2004; 91:1308–1315. [PubMed: 15365563]

Carrano AC, Eytan E, Hershko A, Pagano M. SKP2 is required for ubiquitin-mediated degradation of the CDK inhibitor p27. Nature cell biology. 1999; 1:193–199.

Charafe-Jauffret E, Ginestier C, Monville F, Finetti P, Adelaide J, Cervera N, Fekairi S, Xerri L, Jacquemier J, Birnbaum D, Bertucci F. Gene expression profiling of breast cell lines identifies potential new basal markers. Oncogene. 2006; 25:2273–2284. [PubMed: 16288205]

Clark JP, Cooper CS. ETS gene fusions in prostate cancer. Nat Rev Urol. 2009; 6:429–439. [PubMed: 19657377]

Cowley DO, Graves BJ. Phosphorylation represses Ets-1 DNA binding by reinforcing autoinhibition. Genes Dev. 2000; 14:366–376. [PubMed: 10673508]

Deshaies R. SCF and Cullin/Ring H2-based ubiquitin ligases. Annu Rev Cell Dev Biol. 1999; 15:435–467. [PubMed: 10611969]

Elsberger B, Tan BA, Mitchell TJ, Brown SB, Mallon EA, Tovey SM, Cooke TG, Brunton VG, Edwards J. Is expression or activation of Src kinase associated with cancer-specific survival in ER-, PR- and HER2-negative breast cancer patients? Am J Pathol. 2009; 175:1389–1397. [PubMed: 19762712]

Finn RS, Bengala C, Ibrahim N, Roche H, Sparano J, Strauss L, Fairchild J, Sy O, Goldstein LJ. Dasatinib as a single agent in triple-negative breast cancer: results of an open-label phase 2 study. Clin Cancer Res. 2011; 17:6905–6913. [PubMed: 22028489]

Finn RS, Dering J, Ginther C, Wilson CA, Glaspy P, Tchekmedyian N, Slamon DJ. Dasatinib, an orally active small molecule inhibitor of both the src and abl kinases, selectively inhibits growth of basal-type/“triple-negative” breast cancer cell lines growing in vitro. Breast Cancer Res Treat. 2007; 105:319–326. [PubMed: 17268817]

Hahne JC, Okuducu AF, Kaminski A, Florin A, Soncin F, Wernert N. Ets-1 expression promotes epithelial cell transformation by inducing migration, invasion and anchorage-independent growth. Oncogene. 2005; 24:5384–5388. [PubMed: 15940256]

Herold C, Chadaram V, Peterson B, Marcom P, Hopkins J, Kimmick G, Favaro J, Hamilton E, Welch R, Bacus S, Blackwell K. Phase II trial of dasatinib in patients with metastatic breast cancer using real-time pharmacodynamic tissue biomarkers of Src inhibition to escalate dosing. Clin Cancer Res. 2011; 17:6061–6070. [PubMed: 21810917]

Hirsch HA, Iliopoulos D, Tsichlis PN, Struhl K. Metformin selectively targets cancer stem cells, and acts together with chemotherapy to block tumor growth and prolong remission. Cancer research. 2009; 69:7507–7511. [PubMed: 19752085]

Huang F, Reeves K, Han X, Fairchild C, Platero S, Wong TW, Lee F, Shaw P, Clark E. Identification of candidate molecular markers predicting sensitivity in solid tumors to dasatinib: rationale for patient selection. Cancer research. 2007; 67:2226–2238. [PubMed: 17332353]

Iliopoulos D, Hirsch HA, Struhl K. An epigenetic switch involving NF-kappaB, Lin28, Let-7 MicroRNA, and IL6 links inflammation to cell transformation. Cell. 2009; 139:693–706. [PubMed: 19878981]

Ivan M, Kondo K, Yang H, Kim W, Valiando J, Ohh M, Salic A, Asara J, Lane W, Kaelin WJ. HIFalpha targeted for VHL-mediated destruction by proline hydroxylation: implications for O2 sensing. Science. 2001; 292:464–468. [PubMed: 11292862]

Jaakkola P, Mole D, Tian Y, Wilson M, Gielbert J, Gaskell S, Kriegsheim A, Hebestreit H, Mukherji M, Schofield C, Maxwell P, Pugh C, Ratcliffe P. Targeting of HIF-alpha to the von Hippel-Lindau ubiquitylation complex by O2-regulated prolyl hydroxylation. Science. 2001; 292:468–472. [PubMed: 11292861]

Kumar-Sinha C, Tomlins SA, Chinnaiyan AM. Recurrent gene fusions in prostate cancer. Nat Rev Cancer. 2008; 8:497–511. [PubMed: 18563191]

Kurebayashi J, Kanomata N, Moriya T, Kozuka Y, Watanabe M, Sonoo H. Preferential antitumor effect of the Src inhibitor dasatinib associated with a decreased proportion of aldehyde dehydrogenase 1-positive cells in breast cancer cells of the basal B subtype. BMC Cancer. 2010; 10:568. [PubMed: 20959018]

Lehmann BD, Bauer JA, Chen X, Sanders ME, Chakravarthy AB, Shyr Y, Pietenpol JA. Identification of human triple-negative breast cancer subtypes and preclinical models for selection of targeted therapies. J Clin Invest. 2011; 121:2750–2767. [PubMed: 21633166]

Levy D, Adamovich Y, Reuven N, Shaul Y. Yap1 phosphorylation by c-Abl is a critical step in selective activation of proapoptotic genes in response to DNA damage. Mol Cell. 2008; 29:350–361. [PubMed: 18280240]

Lincoln DW 2nd, Bove K. The transcription factor Ets-1 in breast cancer. Front Biosci. 2005; 10:506–511. [PubMed: 15574387]

Lindemann RK, Braig M, Ballschmieter P, Guise TA, Nordheim A, Dittmer J. Protein kinase Calpha regulates Ets1 transcriptional activity in invasive breast cancer cells. Int J Oncol. 2003; 22:799–805. [PubMed: 12632071]

Lipkowitz S, Weissman AM. RINGs of good and evil: RING finger ubiquitin ligases at the crossroads of tumour suppression and oncogenesis. Nat Rev Cancer. 2011; 11:629–643. [PubMed: 21863050]

Marine JC. Spotlight on the role of COP1 in tumorigenesis. Nat Rev Cancer. 2012; 12:455–464. [PubMed: 22673153]

Matheu A, Maraver A, Serrano M. The Arf/p53 pathway in cancer and aging. Cancer research. 2008; 68:6031–6034. [PubMed: 18676821]

Mayer EL, Baurain J, Sparano J, Strauss L, Campone M, Fumoleau P, Rugo H, Awada A, Sy O, Liombart-Cussac A. A phase 2 trial of dasatinib in patients with advanced HER2-positive and/or hormone receptor-positive breast cancer. Clin Cancer Res. 2011; 17:6897–6904. [PubMed: 21903773]

Mayer EL, Krop IE. Advances in targeting SRC in the treatment of breast cancer and other solid malignancies. Clin Cancer Res. 2010; 16:3526–3532. [PubMed: 20634194]

Mayya V, Lundgren DH, Hwang SI, Rezaul K, Wu L, Eng JK, Rodionov V, Han DK. Quantitative phosphoproteomic analysis of T cell receptor signaling reveals system-wide modulation of protein-protein interactions. Sci Signal. 2009; 2:ra46. [PubMed: 19690332]

Migliorini D, Bogaerts S, Defever D, Vyas R, Denecker G, Radaelli E, Zwolinska A, Depaepe V, Hochepied T, Skarnes WC, Marine JC. Cop1 constitutively regulates c-Jun protein stability and functions as a tumor suppressor in mice. J Clin Invest. 2011; 121:1329–1343. [PubMed: 21403399]

Murphy DA, Courtneidge SA. The ‘ins’ and ‘outs’ of podosomes and invadopodia: characteristics, formation and function. Nature reviews Molecular cell biology. 2011; 12:413–426.

Myers E, Hill AD, Kelly G, McDermott EW, O'Higgins NJ, Buggy Y, Young LS. Associations and interactions between Ets-1 and Ets-2 and coregulatory proteins, SRC-1, AIB1, and NCoR in breast cancer. Clin Cancer Res. 2005; 11:2111–2122. [PubMed: 15788656]

Mylona EE, Alexandrou PT, Giannopoulou IA, Rafailidis PI, Markaki S, Keramopoulos A, Nakopoulou LL. Study of the topographic distribution of ets-1 protein expression in invasive

breast carcinomas in relation to tumor phenotype. Cancer Detect Prev. 2006; 30:111–117. [PubMed: 16632244]

Pognonec P, Boulukos KE, Gesquiere JC, Stehelin D, Ghysdael J. Mitogenic stimulation of thymocytes results in the calcium-dependent phosphorylation of c-ets-1 proteins. The EMBO journal. 1988; 7:977–983. [PubMed: 3136014]

Qin JY, Zhang L, Clift KL, Hulur I, Xiang AP, Ren BZ, Lahn BT. Systematic comparison of constitutive promoters and the doxycycline-inducible promoter. PloS one. 2010; 5:e10611. [PubMed: 20485554]

Rabault B, Ghysdael J. Calcium-induced phosphorylation of ETS1 inhibits its specific DNA binding activity. The Journal of biological chemistry. 1994; 269:28143–28151. [PubMed: 7961750]

Reginato MJ, Mills KR, Becker EB, Lynch DK, Bonni A, Muthuswamy SK, Brugge JS. Bim regulation of lumen formation in cultured mammary epithelial acini is targeted by oncogenes. Molecular and cellular biology. 2005; 25:4591–4601. [PubMed: 15899862]

Sanchez-Bailon MP, Calcabrini A, Gomez-Dominguez D, Morte B, Martin-Forero E, Gomez-Lopez G, Molinari A, Wagner KU, Martin-Perez J. Src kinases catalytic activity regulates proliferation, migration and invasiveness of MDA-MB-231 breast cancer cells. Cell Signal. 2012; 24:1276–1286. [PubMed: 22570868]

Savio MG, Rotondo G, Maglie S, Rossetti G, Bender JR, Pardi R. COP1D, an alternatively spliced constitutive photomorphogenic-1 (COP1) product, stabilizes UV stress-induced c-Jun through inhibition of full-length COP1. Oncogene. 2008; 27:2401–2411. [PubMed: 17968316]

Sherr CJ. Divorcing ARF and p53: an unsettled case. Nat Rev Cancer. 2006; 6:663–673. [PubMed: 16915296]

Singh S, Darnay BG, Aggarwal BB. Site-specific tyrosine phosphorylation of IkappaBalpha negatively regulates its inducible phosphorylation and degradation. The Journal of biological chemistry. 1996; 271:31049–31054. [PubMed: 8940099]

Span PN, Manders P, Heuvel JJ, Thomas CM, Bosch RR, Beex LV, Sweep CG. Expression of the transcription factor Ets-1 is an independent prognostic marker for relapse-free survival in breast cancer. Oncogene. 2002; 21:8506–8509. [PubMed: 12466970]

Summy JM, Gallick GE. Src family kinases in tumor progression and metastasis. Cancer Metastasis Rev. 2003; 22:337–358. [PubMed: 12884910]

Sutterluty H, Chatelain E, Marti A, Wirbelauer C, Senften M, Muller U, Krek W. p45SKP2 promotes p27Kip1 degradation and induces S phase in quiescent cells. Nature cell biology. 1999; 1:207–214.

Tryfonopoulos D, Walsh S, Collins DM, Flanagan L, Quinn C, Corkery B, McDermott EW, Evoy D, Pierce A, O'Donovan N, Crown J, Duffy MJ. Src: a potential target for the treatment of triple-negative breast cancer. Ann Oncol. 2011; 22:2234–2240. [PubMed: 21357651]

Tsvetkov LM, Yeh KH, Lee SJ, Sun H, Zhang H. p27(Kip1) ubiquitination and degradation is regulated by the SCF(Skp2) complex through phosphorylated Thr187 in p27. Curr Biol. 1999; 9:661–664. [PubMed: 10375532]

Vetter M, Blumenthal SG, Lindemann RK, Manns J, Wesselborg S, Thomssen C, Dittmer J. Ets1 is an effector of protein kinase Calpha in cancer cells. Oncogene. 2005; 24:650–661. [PubMed: 15531915]

Vitari AC, Leong KG, Newton K, Yee C, O'Rourke K, Liu J, Phu L, Vij R, Ferrando R, Couto SS, Mohan S, Pandita A, Hongo JA, Arnott D, Wertz IE, Gao WQ, French DM, Dixit VM. COP1 is a tumour suppressor that causes degradation of ETS transcription factors. Nature. 2011; 474:403–406. [PubMed: 21572435]

Wei W, Kaelin WG Jr. Good COP1 or bad COP1? In vivo veritas. J Clin Invest. 2011; 121:1263–1265. [PubMed: 21403396]

Wiederschain D, Wee S, Chen L, Loo A, Yang G, Huang A, Chen Y, Caponigro G, Yao YM, Lengauer C, Sellers WR, Benson JD. Single-vector inducible lentiviral RNAi system for oncology target validation. Cell Cycle. 2009; 8:498–504. [PubMed: 19177017]

Yu JC, Chen JR, Lin CH, Zhang G, Lam PS, Wenger KH, Mozaffari FB, Huang ST, Borke JL. Tensile strain-induced Ets-2 phosphorylation by CaMKII and the homeostasis of cranial sutures. Plast Reconstr Surg. 2009; 123:83S–93S. [PubMed: 19182667]

Zhang Y, Yan LX, Wu QN, Du ZM, Chen J, Liao DZ, Huang MY, Hou JH, Wu QL, Zeng MS, Huang WL, Zeng YX, Shao JY. miR-125b is methylated and functions as a tumor suppressor by regulating the ETS1 proto-oncogene in human invasive breast cancer. Cancer research. 2011; 71:3552–3562. [PubMed: 21444677]

Zhao B, Li L, Tumaneng K, Wang CY, Guan KL. A coordinated phosphorylation by Lats and CK1 regulates YAP stability through SCF(beta-TRCP). Genes Dev. 2010; 24:72–85. [PubMed: 20048001]

Zhao J, Guan JL. Signal transduction by focal adhesion kinase in cancer. Cancer Metastasis Rev. 2009; 28:35–49. [PubMed: 19169797]

Significance

The COP1 ubiquitin ligase complex is lost in some cancers. It is therefore critical to identify COP1 substrates and to understand how COP1 activity is regulated. We discovered that the ETS1 and ETS2 oncogenic transcription factors are COP1 substrates, but only after they are phosphorylated on specific serine or threonine residues occupied by aspartic acid or glutamic acid residues in the canonical COP1 substrates identified to date. Moreover, phosphorylation of a tyrosine residue in ETS1 to its COP1-binding site by Src family kinases allows ETS1 to escape recognition by COP1. These studies expand the universe of potential COP1 substrates, illustrate how kinases can positively or negatively affect degrons recognized by COP1, and provide additional insights into cellular transformation by Src.

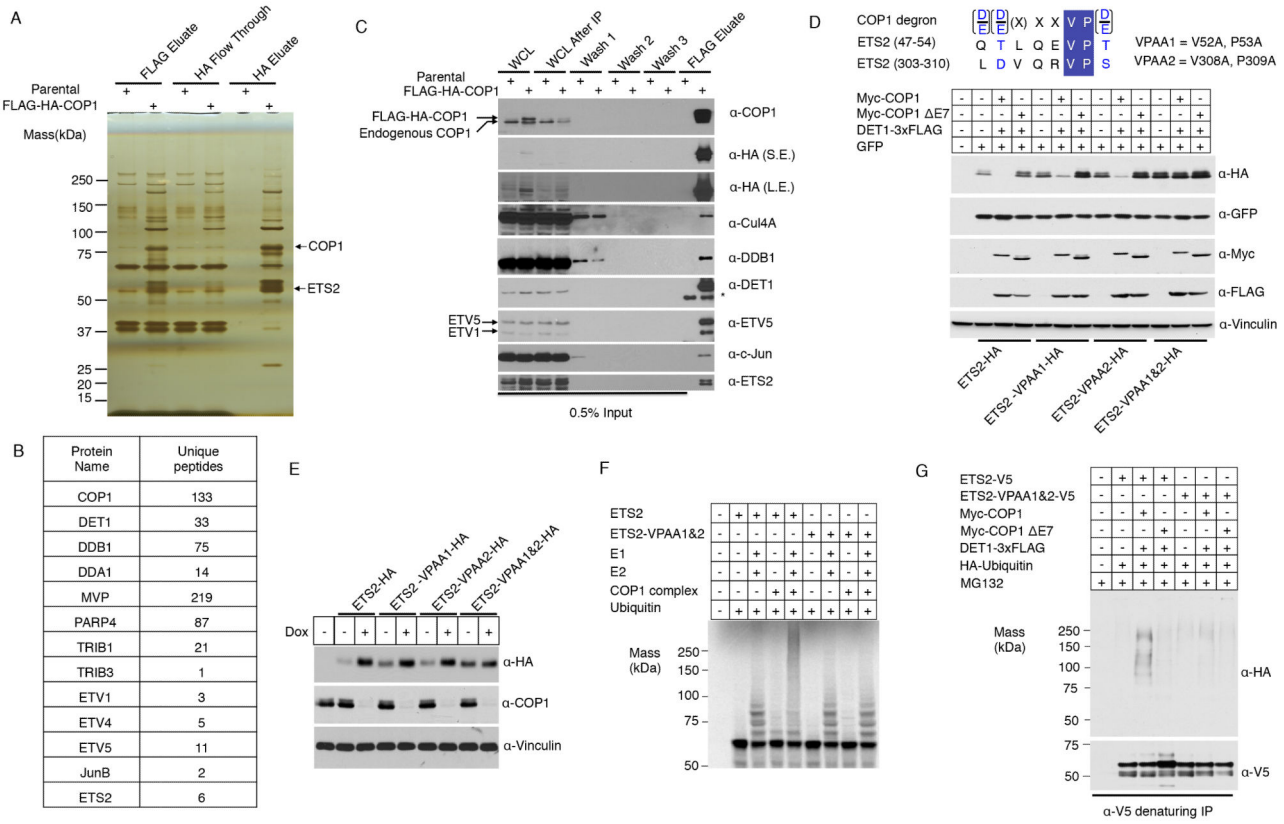

Figure 1. ETS2 is a COP1 Substrate

(A) Silver stained gel of proteins recovered after sequential immunoprecipitation (anti-FLAG followed by anti-HA) of cell extracts prepared from HCT116 colorectal cancer cells (parental or producing FLAG-HA-COP1). Proteins captured with the anti-FLAG antibody were eluted with Flag peptide (FLAG eluate) and applied to an anti-HA column, followed by elution with HA peptide (HA eluate). Shown are proteins present in the FLAG eluate, anti-HA flow-through and HA eluate.

(B) Proteins identified in immunopurified COP1 complex by mass spectrometry.

(C) Immunoblot analysis of proteins recovered after initial anti-FLAG immunoprecipitation and peptide elution as in (A). WCL, whole cell lysate; *, IgG; S.E., short exposure; L.E., long exposure.

(D) Immunoblot analysis of 293FT cells transiently transfected with plasmids encoding the indicated 3xHA-tagged ETS2 variants and, where indicated, DET1 and COP1 (wild-type or dominant-negative AE7). A plasmid encoding GFP was included as a transfection efficiency control.

(E) Immunoblot analysis of 293FT cells expressing a DOX-inducible COP1 shRNA and the indicated HA-tagged ETS2 variants. Cells were treated with or without DOX (1 μg/mL) for 48 hours.

(F) In vitro ubiquitylation of 35S-ETS2 (wild-type or VPAA1&2) in the presence of recombinant E1 and E2 (UbcH5a) and immunopurified COP1.

(G) Anti-HA immunoblot analysis of ETS2-V5 (wild-type or VPAA1&2) that was immunoprecipitated under denaturing conditions from 293FT cells that were transiently transfected with plasmids encoding the indicated proteins.
See also Figure S1.

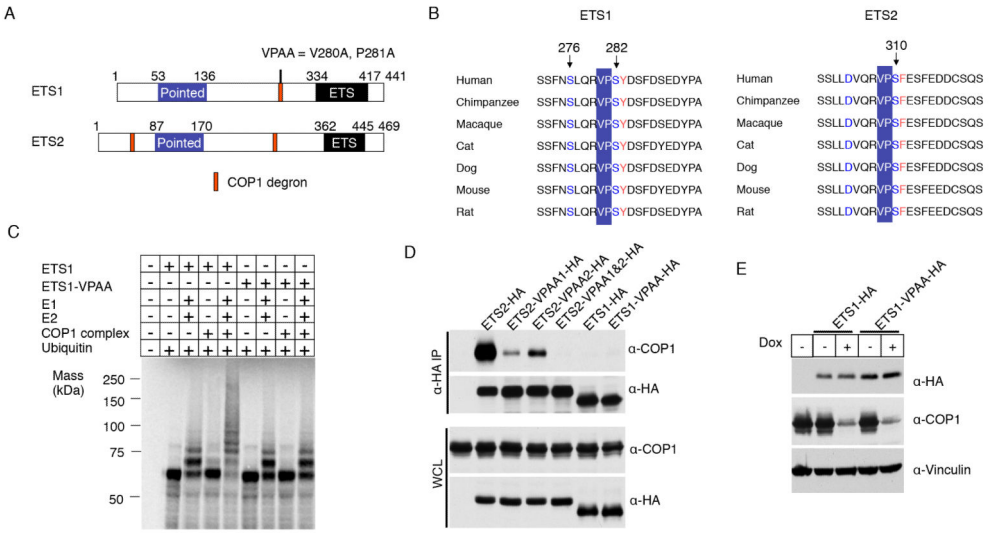

Figure 2. Differential Regulation of ETS1 and ETS2 by COP1

(A) Schematics of ETS1 and ETS2.

(B) Alignments of COP1 degrons in ETS1 and ETS2 (C-terminal site) across species.

(C) In vitro ubiquitylation of ^{35}S-ETS1 (wild-type or VPAA) in the presence of recombinant E1 and E2 (UbcH5a) and immunopurified COP1.

(D) Immunoblot analysis of anti-HA immunoprecipitates from 293FT cells producing the indicated HA-tagged ETS1 and ETS2 variants. Cells were treated with 10 μM MG132 6 hours before harvest.

(E) Immunoblot analysis of 293FT cells expressing a DOX-inducible COP1 shRNA and the indicated 3xHA-tagged ETS1 variants. Cells were treated with or without DOX (1 μg/mL) for 48 hours.

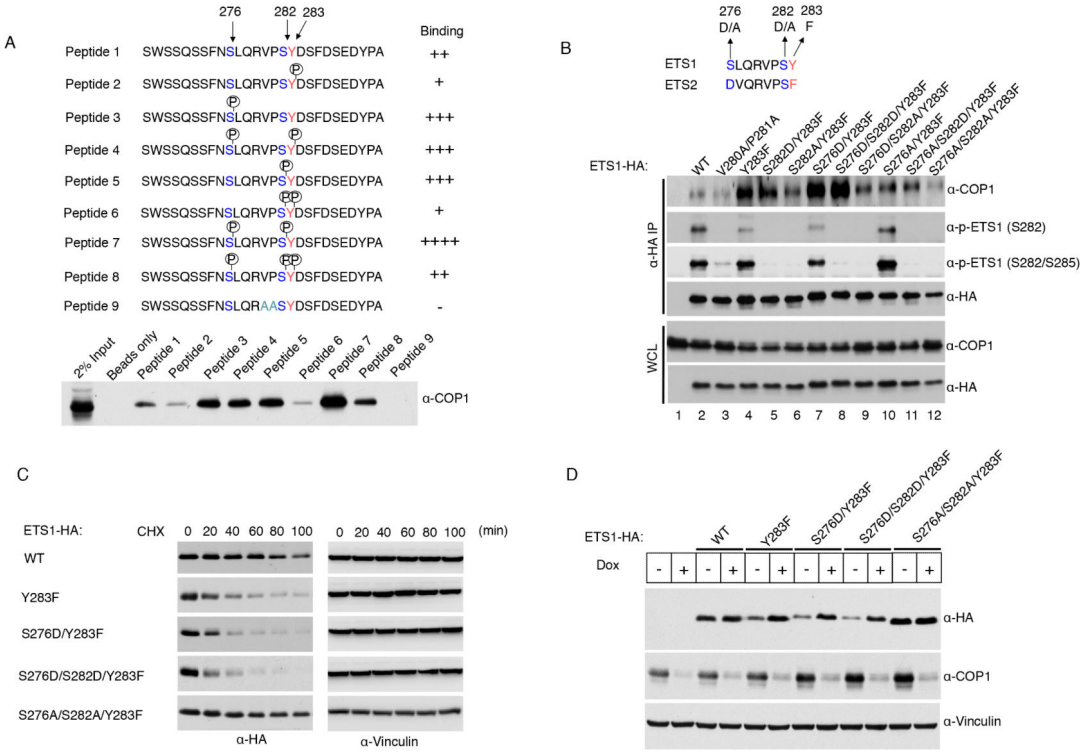

Figure 3. Phosphorylation of ETS1 Governs its Recognition by COP1

(A) Immunoblot analysis of COP1 recovered from 293FT cell extracts after incubation with NeutraAvidin beads loaded with the indicated peptides.

(B) Immunoblot analysis of anti-HA immunoprecipitates from 293FT cells producing the indicated 3xHA-tagged ETS1 variants. Cells were treated with 10 μM MG132 6 hours before harvest.

(C) Immunoblot analysis of 293FT cells expressing the indicated 3xHA-ETS1 variants after the addition of 100 μg/mL cyclohexamide (CHX). Different exposure times were used to normalize the 0 minute band intensities for the different ETS1 variants.

(D) Immunoblot analysis of 293FT cells expressing a DOX-inducible COP1 shRNA and the indicated 3xHA-tagged ETS1 variants. Cells were treated with or without DOX (1 μg/mL) for 48 hours.

See also Figure S2.

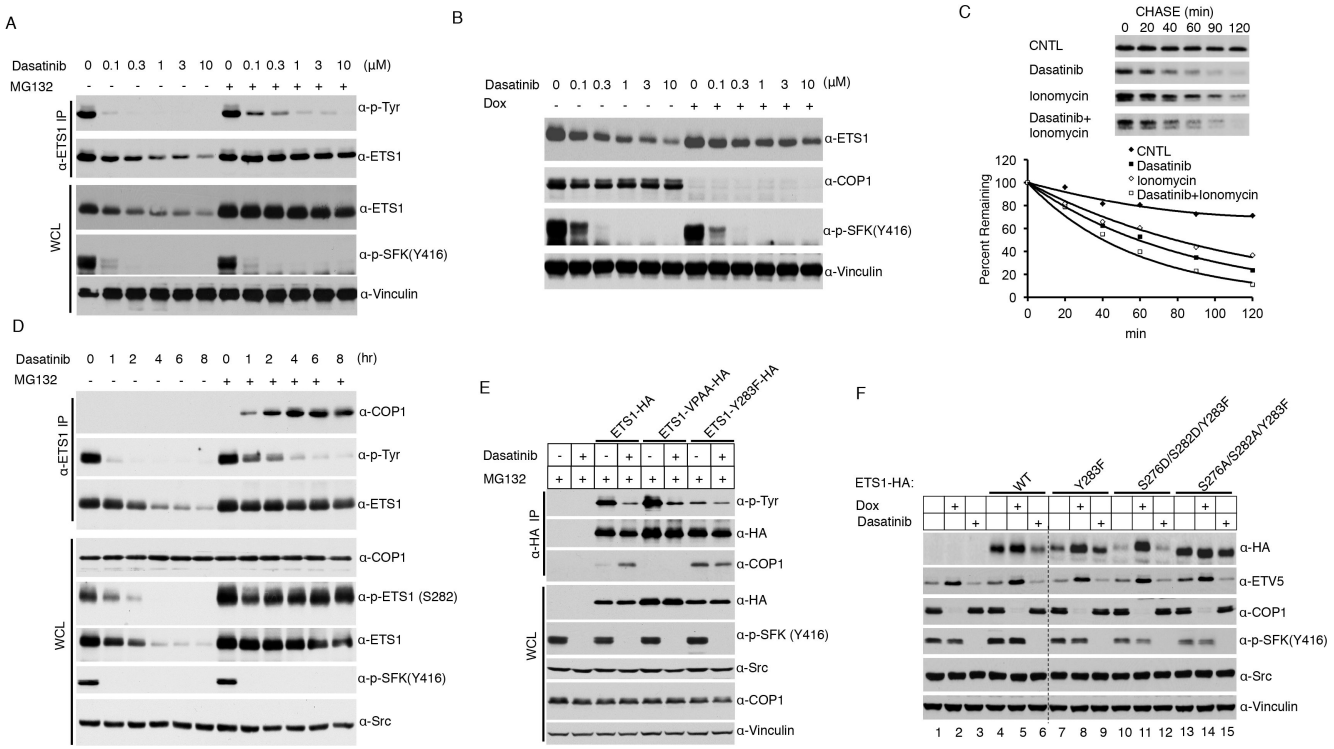

Figure 4. Dasatinib Downregulates ETS1

(A and B) Immunoblot analysis of anti-ETS1 immunoprecipitates or whole cell extracts of MDA-MB-231 cells expressing a DOX-inducible COP1 shRNA treated with increased amounts of dasatinib for 8 hours with or without pretreatment of MG132 (10 μM) for 2 hours (A) or Dox (1μg/mL) for 48 hours (B).

(C) ^{35}S Pulse-chase analysis of ETS1 recovered from MDA-MB-231 cells pretreated with dasatinib (10 μM) for 3 hours and/or ionomycin (2 μM) for 0.5 hours. MDA-MB-231 cells treated with DMSO were used as a control (CNTL).

(D) Immunoblot analysis of anti-ETS1 immunoprecipitates or whole cell extracts of MDA-MB-231 cells at the indicated timepoints after addition of dasatinib (10 μM). Where indicated cells were pretreated with MG132 (10 μM) for 2 hours.

(E) Immunoblot analysis of anti-HA immunoprecipitates or whole cell extracts of MDA-MB-231 cells producing the indicated 3xHA-tagged ETS1 variants pretreated with MG132 (10 μM) for 2 hours and, where indicated, with dasatinib (10 μM), for an additional 8 hours.

(F) Immunoblot analysis of MDA-MB-231 cells expressing a DOX-inducible COP1 shRNA and the indicated HA-tagged ETS1 variants. Where indicated cells were pretreated with Dox (1μg/ml) for 48 hours and dasatinib (10 μM) for an additional 8 hours. Dotted line indicates where irrelevant lanes were removed from the blot image..

See also Figure S3.

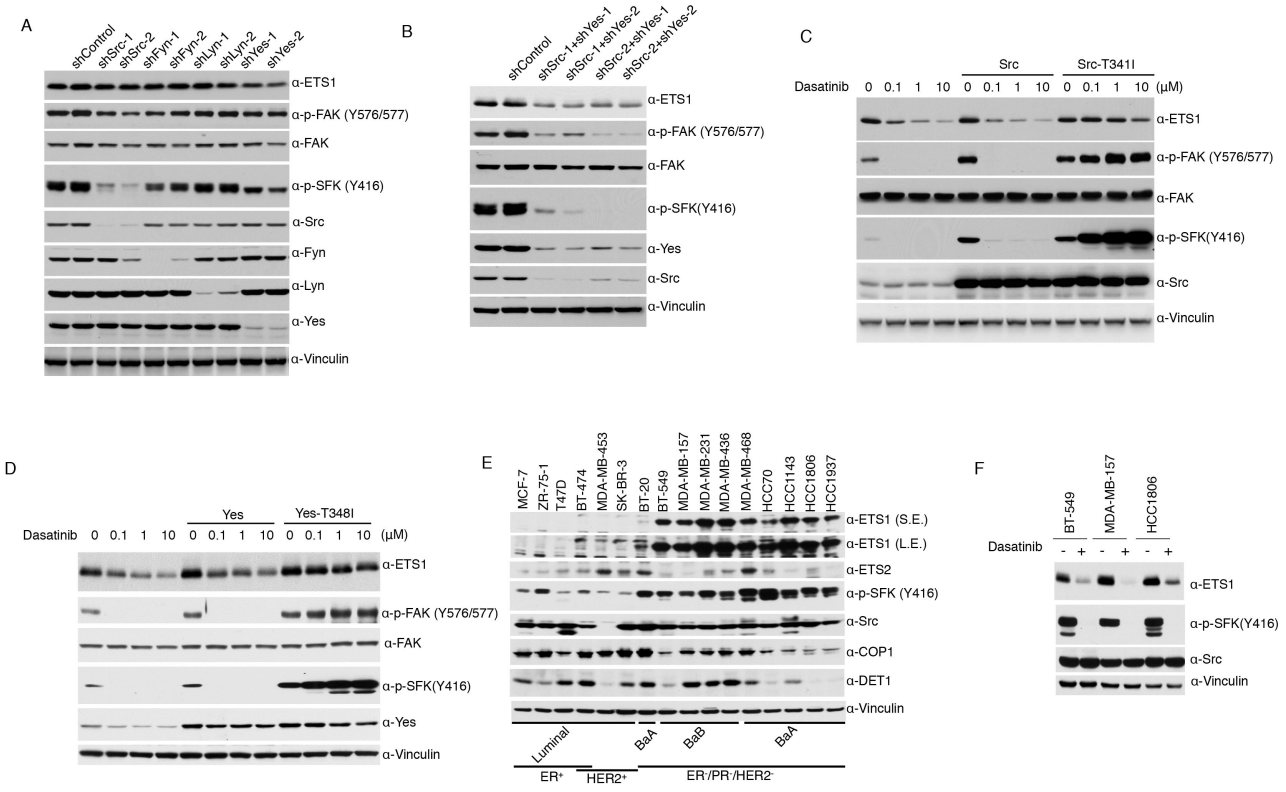

Figure 5. Src and Yes Redundantly Control ETS1 Stability

(A and B) Immunoblot analysis of MDA-MB-231 cells expressing the indicated shRNAs.

(C and D) Immunoblot analysis of MDA-MB-231 cells expressing the indicated Src (C) or Yes (D) variants and treated, where indicated, with dasatinib.

(E and F) Immunoblot of the indicated breast cancer cell lines. BaA = Basal A subtype. BaB = Basal B subtype. Dasatinib (1μM) was added for 8 hours where indicated in (F). S.E., short exposure. L.E., long exposure.

See also Figure S4.

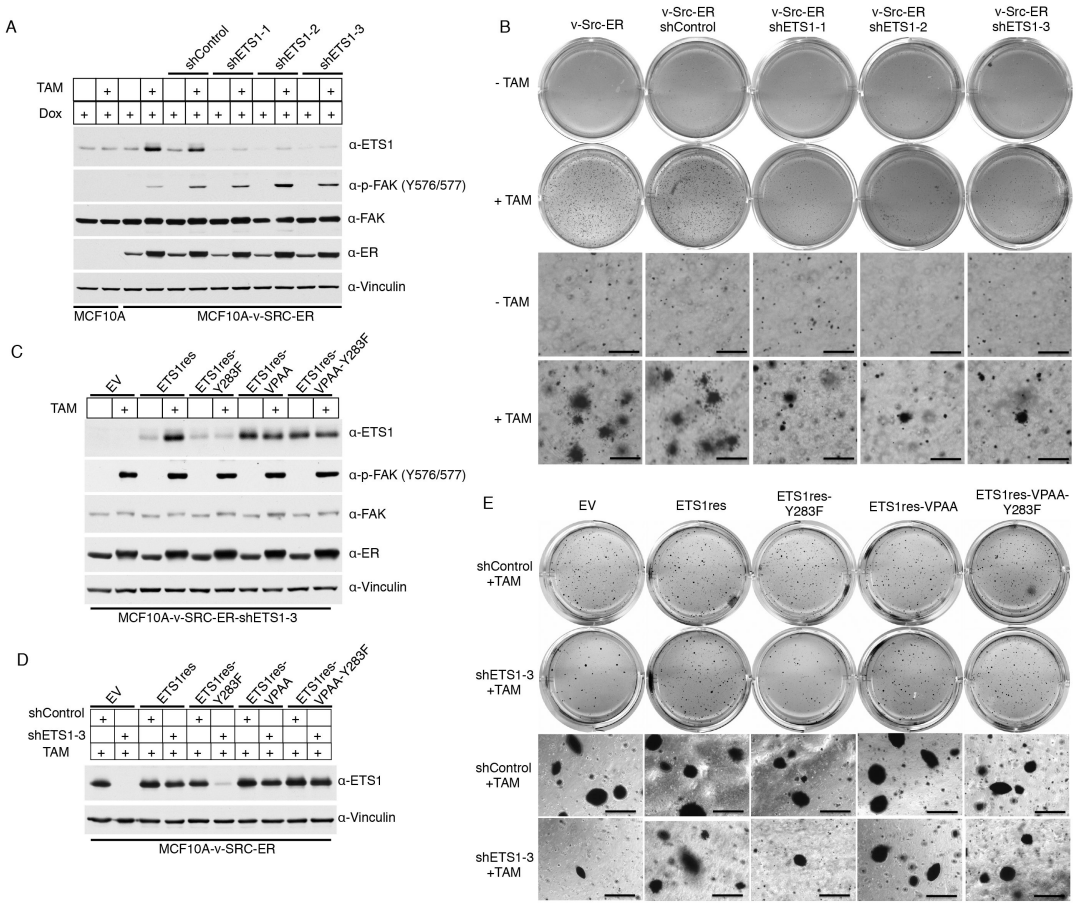

Figure 6. Role of Src and ETS1 in Mammary Transformation

(A and B) Immunoblot analysis (A) and soft agar assay (B) of MCF10A cells expressing a v-Src-ER fusion protein and the indicated DOX-inducible shRNAs. Cells were grown in the presence of DOX (1 μg/mL). 4-OH-tamoxifen (TAM, 1μg/ml) was also added where indicated. Parental MCF10A were included in (A) as a control. Scale bars, 0.5 mm.

(C, D and E) Immunoblot analysis (C and D) and soft agar assay (E) of MCF10A-v-Src-ER cells stably expressing control shRNA (shControl) or shRNA against ETS1 (shETS1-3) and indicated shRNA-resistant (res) ETS1 cDNAs. Cells were treated with vehicle or 4-OH-tamoxifen (1μg/ml) for 12 hours where indicated. Scale bars, 0.5 mm. Representative images shown in (B) and (E) are from three biological replicates.

See also Figure S5.

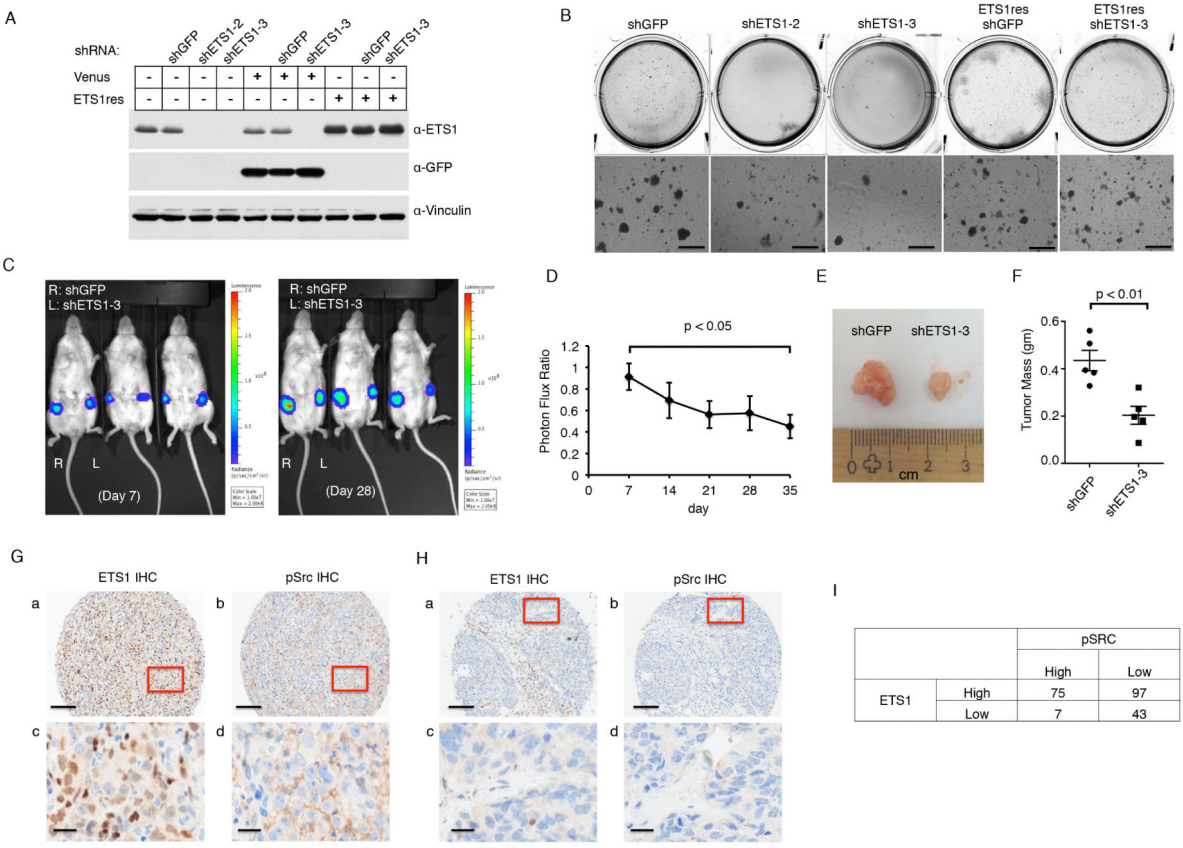

Figure 7. ETS1 Promotes Tumor Growth in Human Triple Negative Breast Cancer

(A and B) Immunoblot analysis (A) and soft agar assay (B) of MDA-MB-231 cells stably expressing shRNAs against GFP or ETS1 (shRNA 2 or 3) and, where indicated, an mRNA encoding venus fluorescent protein (Venus) or an shRNA-resistant (for shRNA 3) mRNA encoding ETS1 (ETS1res). Representative images in (B) are from three biological replicates.

(C, D) Representative bioluminescent images of mice orthotopically injected with MDA-MB-231 cells stably expressing firefly luciferase cDNA and the indicated shRNAs (C) and quantification of shEST1-3/shGFP signal ratios at the indicated time (D, n=5). Error bar represents SEM.

(E and F) Representative appearance of tumors (E) and mean tumor mass (F) at necropsy. Error bar indicates SEM.

(G and H) Representative images of breast cancer tumors with high (G) or low (H) levels of ETS1 and phospho-Tyr416 Src detected by immunohistochemistry. Red solid box in (a) and (b) are magnified in (c) and (d), respectively. Scale bars in (a) and (b) represent 100 μM; Scale bars in (c) and (d) represent 20 μM.

(I) The classification of tumor cores based upon the level of ETS1 and phospho-Tyr416 Src. See also Figure S6 and Table S1.